

## The Alpujarride–Nevado-Filábride extensional shear zone, Betic Cordillera, SE Spain

ANTONIO JABALOY, JESÚS GALINDO-ZALDÍVAR and FRANCISCO GONZÁLEZ-LODEIRO

Dpto de Geodinámica, I.A.G.M., Universidad de Granada, C.S.I.C. 18071, Granada, Spain

(Received 30 December 1991; accepted in revised form 8 September 1992)

**Abstract**—In the Betic Cordillera, the initial thickening of the Alborán Domain produced an Alpine high pressure–low temperature (HP–LT) metamorphism in the Alpujarride and Nevado-Filábride complexes. After 19 Ma this thickening process evolved to an extensional stage with uplift rates of between 1 and 2 mm year<sup>-1</sup>. The extensional stage generated structures in a heterogeneous shear regime with a top-to-the-west sense of movement. The present-day Alpujarride–Nevado-Filábride contact is a detachment fault generated in this shearing regime. In the footwall, the first structure developed in this extensional stage is a planar-linear fabric characterized by constrictive strain, that is axial planar to kilometric recumbent tight to isoclinal folds. The planar-linear fabric is folded by inclined close to open folds with axes parallel to the stretching lineation. The planar-linear fabric and folds are deformed by a late extensional crenulation cleavage near the detachment surface. Finally, brittle deformation was generated within the same kinematic framework as that of the ductile structures. In the hanging wall, meanwhile, deformation had a brittle character producing faults and joints.

### INTRODUCTION

THE Betic Cordillera contains a northern sector called the External Zones (Fallot 1948) or South-Iberian Domain (García-Dueñas & Balanyá 1986) composed of sedimentary and volcanic rocks that are Mesozoic and Tertiary in age, and which are deformed by folds and thrusts with a northwestwards vergence. A southern sector, called the Internal Zones (Fallot 1948) or Alborán Domain (García-Dueñas & Balanyá 1986) is composed of metamorphic and sedimentary rocks

grouped in several tectonic units. In the western Betic Cordillera, between these sectors, there is also a Campo de Gibraltar Complex (Fallot 1948) made up of several tectonic units with flysch material (Fig. 1).

The tectonic units of the Alborán Domain have been grouped in the following complexes: Dorsalian (Durand-Delgá & Foucault 1967), Predorsalian (Didon *et al.* 1973), Alosaina (Balanyá & García-Dueñas 1987), Maláguide (Blumenthal 1927), Alpujarride (Van Bemelen 1927) and Nevado-Filábride (Egeler 1964) (Fig. 1). The three last complexes constitute the greater part

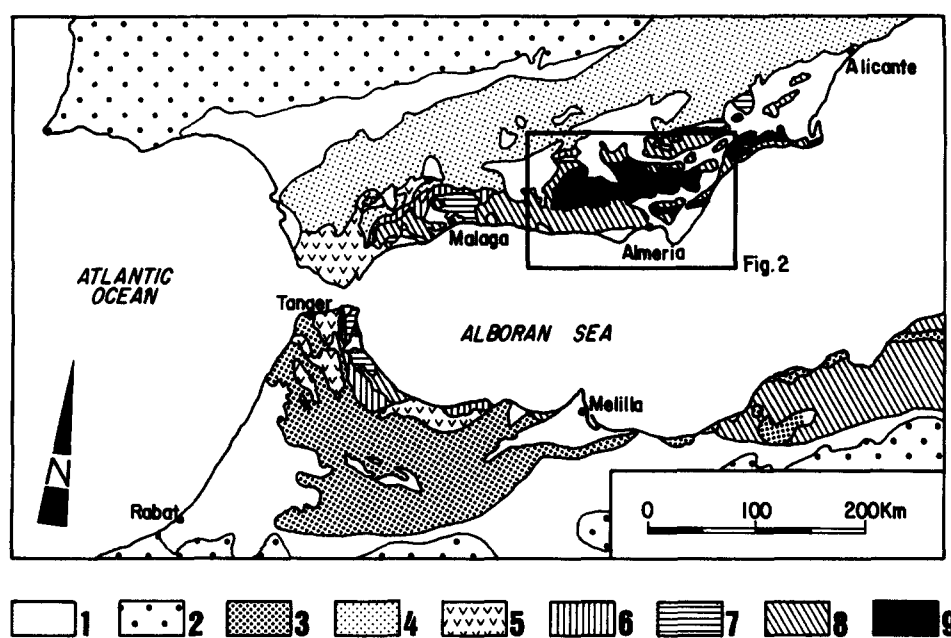


Fig. 1. Geological map of the Betic Cordillera. The Rifian Cordillera is also shown on the African Margin. 1, Neogene sedimentary and volcanic rocks; 2, Hesperian Massif; 3, African–Maghreb Domain; 4, South-Iberian Domain; 5, Campo de Gibraltar Flysch, Alborán Domain; 6, Dorsalian, Predorsalian and Alosaina Complexes; 7, Maláguide Complex; 8, Alpujarride Complex; 9, Nevado-Filábride Complex.

of the outcrops of the domain, and they are superposed, from bottom to top, in the following order: Nevado-Filábride, Alpujárride and Maláguide. The contacts between these complexes had traditionally been interpreted as thrust surfaces (see Egeler & Simon 1969), but more recently they have been interpreted as low-angle normal faults (Aldaya *et al.* 1984, 1991, García-Dueñas *et al.* 1986, Galindo-Zaldívar *et al.* 1989, Platt & Vissers 1989). The Alpujárride–Nevado-Filábride contact is now defined as a brittle fault called the Mecina detachment fault (Galindo-Zaldívar *et al.* 1991). This detachment began to be active under ductile conditions and generated fabrics and folds. Ductile–brittle and brittle structures are superposed over the ductile ones. This sequence of deformation is now well exposed in the footwall (Nevado-Filábride Complex) (Platt & Vissers 1980, Platt *et al.* 1984, Platt & Behrmann 1986, Galindo-Zaldívar *et al.* 1989).

The aim of this paper is to analyse the geometry and kinematics of this detachment, as well as the geometry, spatial distribution and temporal evolution of the ductile and brittle structures developed in the footwall.

## GEOLOGICAL SETTING

The Alpujárride Complex is made up of a stack of tectonic units with an ascending sequence, in the upper units, of: (a) gneisses, graphitic schists and metapsammites assumed to be Precambrian–Palaeozoic in age; (b) metapelites (mainly phyllites) with levels of metapsammites, calc-schists and gypsum, assumed to be Permian–Werfenian in age; (c) carbonate rocks: limestones and dolostones dated as Middle to Upper Triassic. All these rocks suffered a metamorphic event under high pressure–low temperature conditions (HP–LT) with up to 10 kbar of pressure (Goffé *et al.* 1989, Azañón & Goffé 1991). This event evolved to intermediate pressure–intermediate temperature (IP–IT) and low pressure–high temperature (LP–HT) conditions (Torres-Roldán 1979). Monié *et al.* (1991) indicate that the end of the HP–LT metamorphic event in the lower Alpujárride units occurred at 25 Ma and that these rocks cooled below 350°C at 19 Ma.

The Nevado-Filábride Complex is composed of a lower lithological ensemble made up of black schists and metapsammites with levels of black metapelites and carbonates (Montenegro and Aulago Formations; Martínez-Martínez 1985), assumed to be Palaeozoic in age (Lafuste & Pavillon 1976). It also contains an upper lithological ensemble, assumed to be Permian–Mesozoic in age, that is made up from bottom to top by metaconglomerates, metapsammites and grey schists (Tahal Formation, Nijhuis 1964), overlain by marbles, with layers of schists and meta-evaporites (Las Casas Formation, Martínez-Martínez 1985). Within the Tahal and Las Casas Formations are bodies of orthogneisses, metabasites (eclogites and amphibolites), serpentinites and peridotites. In the metabasites, mineral associations with garnet and omphacite are recognized (Nijhuis

1964). In the meta-evaporites there are assemblages with kyanite, phengite and talc (Gómez-Pugnaire & Cámara 1990) indicating HP–LT metamorphic conditions. These mineral associations are transformed to assemblages with amphibole, plagioclase and epidote in the metabasites, and to assemblages with scapolite and phlogopite in the meta-evaporites indicating IP–IT metamorphic conditions (Nijhuis 1964, Gómez-Pugnaire & Cámara 1990).  $^{39}\text{Ar}/^{40}\text{Ar}$  ages (Monié *et al.* 1991) show that the HP–LT alpine metamorphic event ended at 48 Ma; the IP–IT metamorphic event ended at 23 Ma; and the white micas cooled below 350°C at 16 Ma.

## DEFORMATION IN THE NEVADO-FILABRIDE COMPLEX

This complex outcrops below the rocks of the Alpujárride Complex in the core of late antiforms with an E–W trend. The two complexes are separated by the Mecina detachment fault. In the footwall (Nevado-Filábride Complex), a planar-linear fabric ( $S_p/L_p$ ), formed in a heterogeneous ductile shearing regime, is recognized (González-Lodeiro *et al.* 1984, Platt *et al.* 1984).  $S_p/L_p$  together with shear surfaces  $C_p$  define a ductile extensional crenulation cleavage. The planar-linear fabric deforms previous foliations ( $S_i$ ), and it is axial planar to tight to isoclinal recumbent folds ( $F_p$ ) with kilometric amplitudes. It is folded, in turn, by inclined close to open folds ( $F_c$ ) with an associated crenulation cleavage ( $S_c$ ). These  $F_c$  folds are affected by a late extensional crenulation cleavage. The latest structures are high- and low-angle normal faults, systematic joints and gentle to open upright folds.

### *Structures pre-dating the planar-linear fabric*

The intensity of the planar-linear fabric makes the study of the earlier structures difficult. The features of the earlier structures are recognized only in some areas, and they are clearly polyphase in nature. These structures are: a crenulation cleavage in the Sierra Alhamilla (Platt & Behrmann 1986) and in the western Sierra de los Filabres, a first-phase schistosity in the central and eastern Sierra de los Filabres (Langenberg 1972, Vissers 1981), or a slaty cleavage in the lower part of the western Sierra de los Filabres (Jabaloy 1991). The vergence of the folds associated with these fabrics is generally northward in the Sierra de los Filabres (Vissers 1981, Jabaloy 1991), and southward in the lower part of western Sierra de los Filabres. In the central Sierra de los Filabres, these structures were generated in HP–LT metamorphic conditions (Vissers 1981).

### *Planar-linear fabric ( $S_p/L_p$ )*

This fabric generally has low dips. Locally the  $F_c$  folds and latest gentle to open folds deform the  $S_p$  foliation giving greater angles of dip, which are even vertical or locally overturned in the northern Sierra de

los Filabres and northern Sierra Alhamilla. The  $S_p/L_p$  fabric is developed through a broad zone (Figs. 2 and 3) with a thickness that is variable from the east-northeast to the west-southwest: it is about 800 m thick in north-eastern Sierra de los Filabres, and about 2000–2500 m thick in the western Sierra Nevada (Galindo-Zaldívar 1990). The lower boundary of this zone with planar-linear fabric is not a sharp one; there is a progressive downwards decrease in the intensity of the fabric. In certain areas, such as the southern Sierra Alhamilla (Platt & Behrmann 1986) or the western Sierra de los Filabres, this boundary is sometimes a narrow band with a thickness ranging from 1 to 50 m. The lower limit of planar-linear fabric development is oblique to the lithological contacts, a fact that is observed clearly in the eastern Sierra de los Filabres; in this area the bottom of the Tahal Formation is not affected by the planar-linear fabric, whereas the whole formation is affected by it in the western parts of the Sierra de los Filabres. The lithological formations deformed by the planar-linear fabric decrease in thickness from the east-northeast to the west-southwest: i.e. the Tahal Formation has a minimum thickness of 2200 m in the eastern Sierra de los Filabres, and a maximum thickness of 200 m in the western Sierra Nevada (Figs. 2 and 3).

The planar-linear fabric is defined by a schistosity with

a stretching and/or mineral lineation. The intensity of this fabric increases upward. The trend of the stretching lineation is variable and it has a curved pattern between the Sierra Nevada and the Sierra Alhamilla (Fig. 2) (González-Lodeiro *et al.* 1984, Martínez-Martínez 1984, Platt & Behrmann 1986, Galindo-Zaldívar *et al.* 1989, Zevenhuizen 1989, Galindo-Zaldívar 1990, Soto *et al.* 1990, Jabaloy 1991).

The  $S_p/L_p$  fabric is associated with a retrograde metamorphism. The minerals produced during the previous metamorphic events under HP–LT and IP–IT conditions (amphibole, garnet, staurolite, chloritoid, kyanite and other minerals) are deformed by the  $S_p$  schistosity. Mineral associations indicating greenschist facies conditions (quartz + white mica + garnet + albite + chlorite) are syn-kinematic with  $S_p/L_p$  in the lower part of the zone affected by the fabric. The chlorite is really an intergrowth of chlorite, micas and clay minerals (Mellini *et al.* 1991). The garnet of the greenschist facies association is almandine-rich and also has a very high grossularite content. White micas are either phengite with a  $Si^{4+}$  content of about 3.2, or paragonite. Data from the garnet–phengite geothermometer (Krogh & Råheim 1976) and  $Si^{4+}$  content of the phengites (Massone & Schreyer 1987) indicate metamorphic conditions for the formation of the planar-linear fabric of about

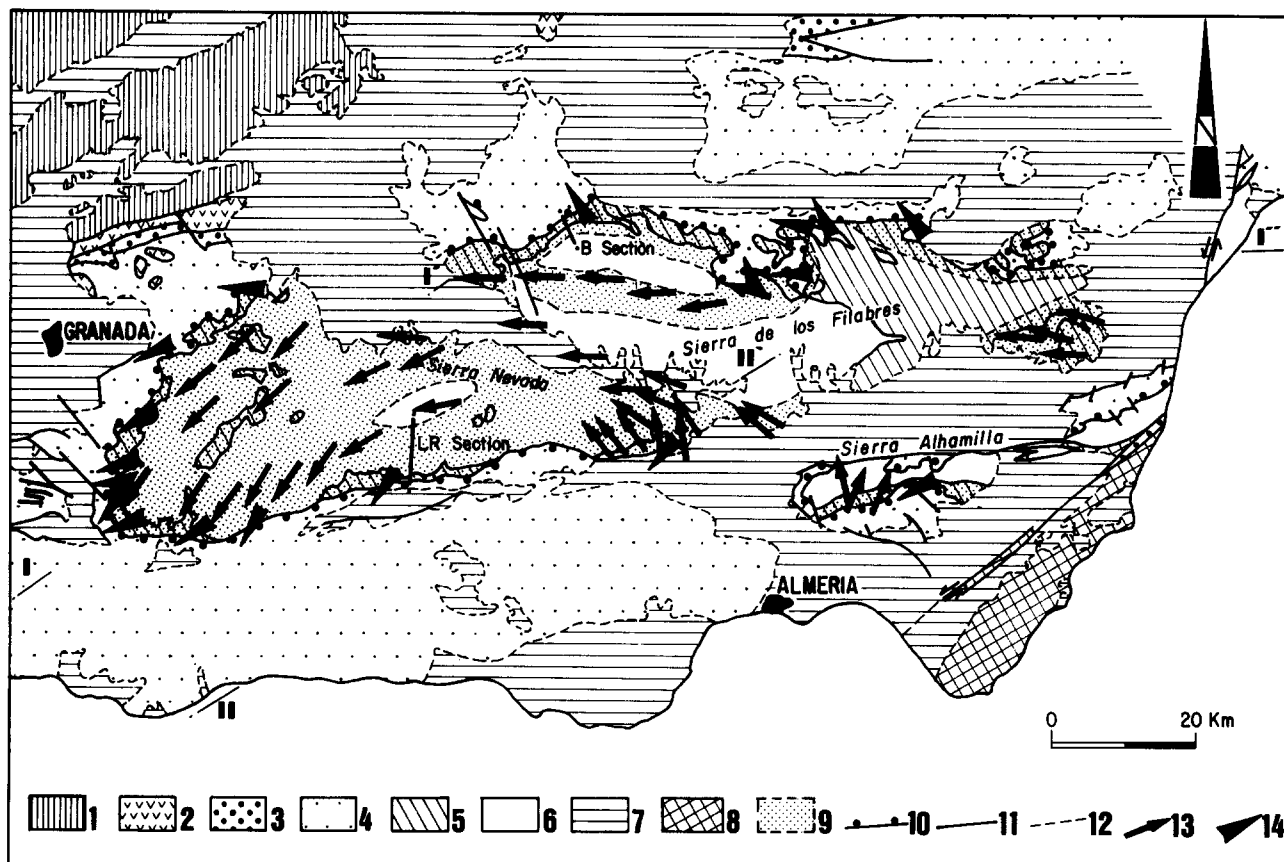


Fig. 2. Distribution of the planar-linear fabric and orientation of the stretching lineation in the Nevado-Filábride Complex (south-eastern Betic Cordillera). 1, South-Iberian Domain, Alborán Domain; 2, Dorsalian Complex; 3, Málagaide Complex; 4, Alpujarride Complex; 5, Nevado-Filábride Complex, Tahal and Las Casas Formations; 6, Nevado-Filábride Complex, Montenegro and Aulago Formations; 7, Neogene and Quaternary sedimentary rocks; 8, Neogene volcanic rocks; 9, planar-linear fabric in the Nevado-Filábride rocks; 10, Mecina detachment fault; 11, faulted contact; 12, unconformity; 13, orientation of the stretching lineation with indication of the sense of movement of the top for the planar-linear fabric; and 14, sense of movement of the hanging wall of the Mecina detachment fault.

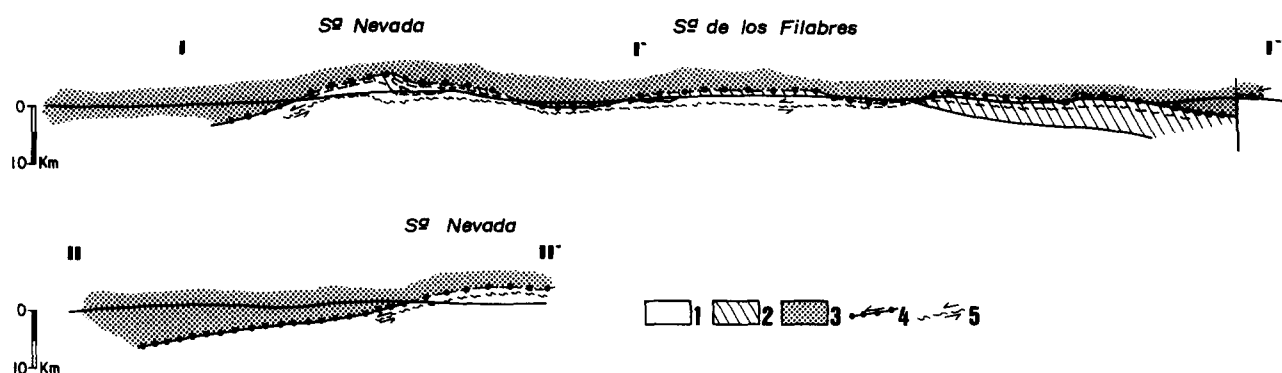


Fig 3. Geological cross-sections of the southeastern Betic Cordillera. Locations are shown in Fig. 2. 1, Nevado-Filábride Complex, Montenegro and Aulago Formations; 2, Nevado-Filábride Complex, Tahal and Las Casas Formations; 3, Alpujárride Complex; 4, Mecina detachment fault; and 5, lower limit of the planar-linear fabric.

$510 \pm 50^\circ\text{C}$  and about  $4.3 \pm 2$  kbar pressure in the western Sierra de los Filabres (Jabaloy 1991). Behrmann (1983) estimated temperatures of around  $300^\circ\text{C}$  from calcite-dolomite geothermometry on marbles from the Sierra Alhamilla, reflecting that the formation of this fabric can occur at different stages during the retrograde metamorphic event.

Kinematic criteria, such as asymmetric quartz  $\langle c \rangle$ -axis fabrics,  $S$ - $C$  structures, ductile extensional crenulation cleavage, asymmetric pressure shadows around previous porphyroblasts and mica-fish indicate that the strain producing the planar-linear fabric has a significant non-coaxial component. These kinematic criteria show generally a top-to-the-west sense of movement for this non-coaxial component of the strain. In several places, which are less common, the same kinematic criteria define a sense of movement of the hanging wall towards the east, whereas additional structures such as symmetric quartz  $\langle c \rangle$ -axis fabrics or symmetric pressure shadows indicate that the strain has in some points, a coaxial component (Galindo-Zaldívar *et al.* 1989).

The measurements of the finite strain made using quartzitic pebbles from a metaconglomerate with quartzitic matrix (Jabaloy & González-Lodeiro 1988), and using the orientations of tourmalines and potassic feldspar porphyroblasts in a deformed orthogneiss (Soto *et al.* 1990), show intermediate to prolate strain ellipsoids with a value for  $k$  of between 1 and 3.5.

Associated with the planar-linear fabric, there are shear surfaces ( $C_p$ ) that define an extensional crenulation cleavage with a ductile character. This extensional crenulation cleavage was described for the first time by Platt & Vissers (1980). The spacing between the shear surfaces, in the lower part of the zone with the  $S_p/L_p$  fabric, is greater than 10 cm, and the angle between the  $C_p$  surfaces and the  $S_p$  foliation is very low. These  $C_p$  surfaces deform the contact between layers of schists and metapsammities with a well developed planar-linear fabric ( $S_p/L_p$ ), but they disappear inside the layers of metapsammite. This fact implies that the planar-linear fabric and  $C_p$  are in part simultaneous (Platt & Vissers 1980). In the western Sierra de los Filabres these surfaces are folded by the  $F_c$  folds.

The quartz microstructures in the quartzofeldspathic rocks vary depending on the distance from the detachment surface (Fig. 4). Furthest away, where the planar-linear fabric is not developed, the detrital grains of quartz and the fabrics generated in previous deformational events are preserved. Approaching the detachment surface, an evolution of the fabrics can be observed: fabrics with elongate grain mosaics, whose grain size increases upwards; fabrics with quartz grains with serrate borders; fabrics with polycrystalline ribbons; fabrics with monocrystalline ribbons; and in the uppermost part, ultramylonitic fabrics with neoformed grains. The vertical variation of the quartz microstructures shows a progressive increase in the strain intensity in an upward sense. This variation is accompanied by a decrease in the temperature of deformation toward the upper part, inferred from the fact that monocrystalline ribbons occur in higher zones than polycrystalline ribbons (Bouiller & Bouchez 1978). Moreover, the minerals of the retrograde greenschist facies associations are syn-kinematic with the planar-linear fabric in the lower parts, and pre-kinematic in the higher parts. These blastesis-deformation relations and the zoning of the quartz microstructures suggest that the fabrics now observed in the higher parts were generated at a lower temperature and are younger than those observed in the lower parts.

The quartz  $\langle c \rangle$ -axis fabrics also vary in a vertical section through the zone with the planar-linear fabric (Fig. 5). In the lowermost areas there are disordered and coaxial fabrics. Upwards, the fabrics develop one or two poorly defined girdles, which further up still become better defined. This evolution is manifested by a decrease in the density of the maxima near the  $X$  axis, and an increase in the density of the maxima around the  $Z$  and  $Y$  axes, and in intermediate positions that correspond to basal and prismatic glide in the  $\langle a \rangle$  direction, and rhombohedral glide. Finally, near the detachment surface, the predominant fabrics develop only one girdle. These fabrics frequently have a sigmoidal shape, with maxima around the  $Y$  axis, and are sometimes poorly defined near the  $Z$  axis.

The planar-linear fabric ( $S_p/L_p$ ) is axial planar to

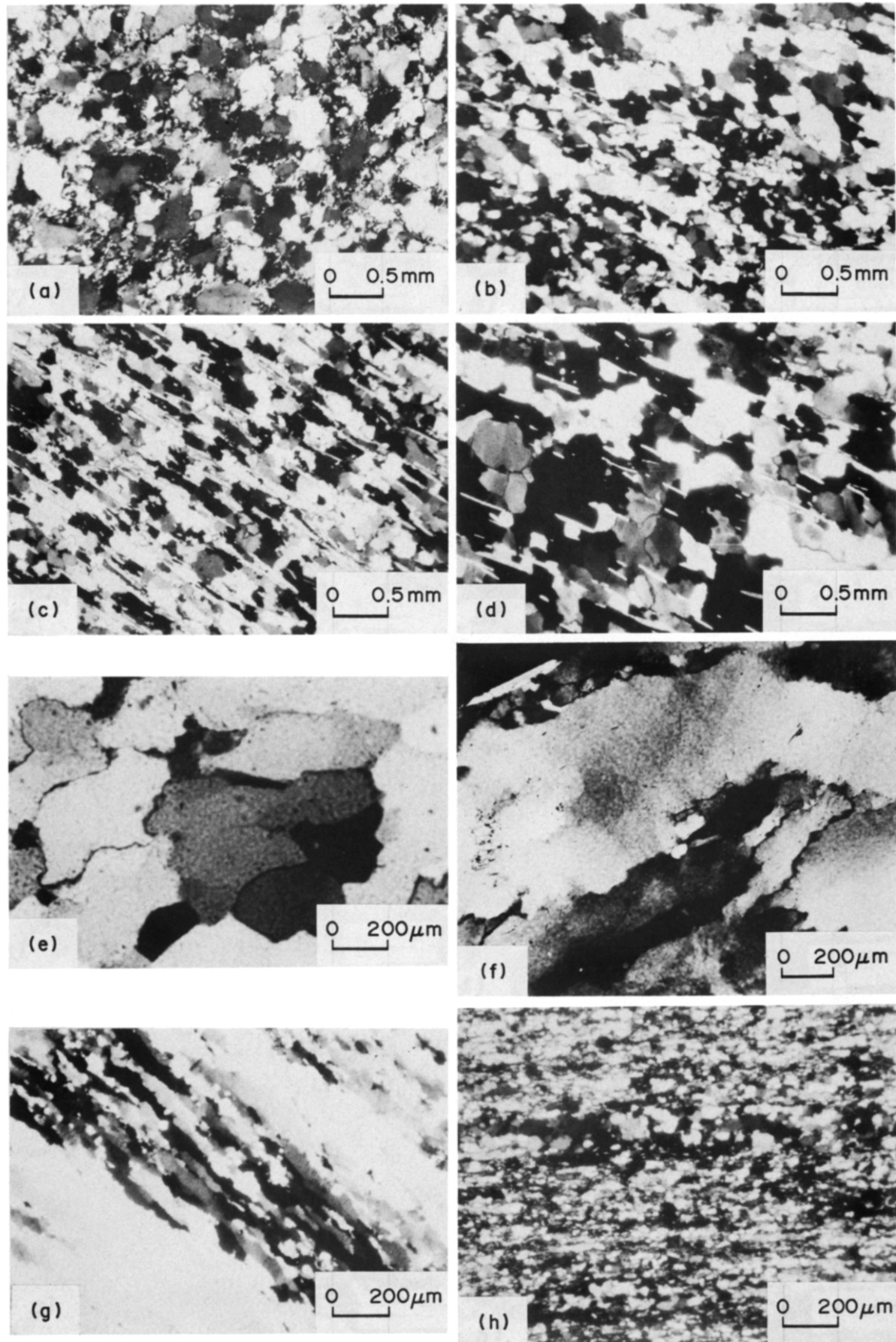


Fig. 4. Quartz microstructures in Nevado-Filábride rocks in a composite vertical section through the zone with planar-linear fabric from (a) (bottom) to (h) (near the detachment fault). Locations are shown in Fig. 2. Rocks of the lower part (a, b, c & d) come from the B section in the western Sierra de los Filabres, rocks of the higher part (e, f, g & h) come from the LR section in the central Sierra Nevada. (a) Detrital quartz grains in a metapsammite without  $S_0/L_0$  fabric. (b), (c) (d) & (e) Elongate mosaic fabrics with increasing grain size. (f) Serrated boundaries. (g) Monocrystalline and polycrystalline ribbons. (h) Ultramylonite with neofomed grains.



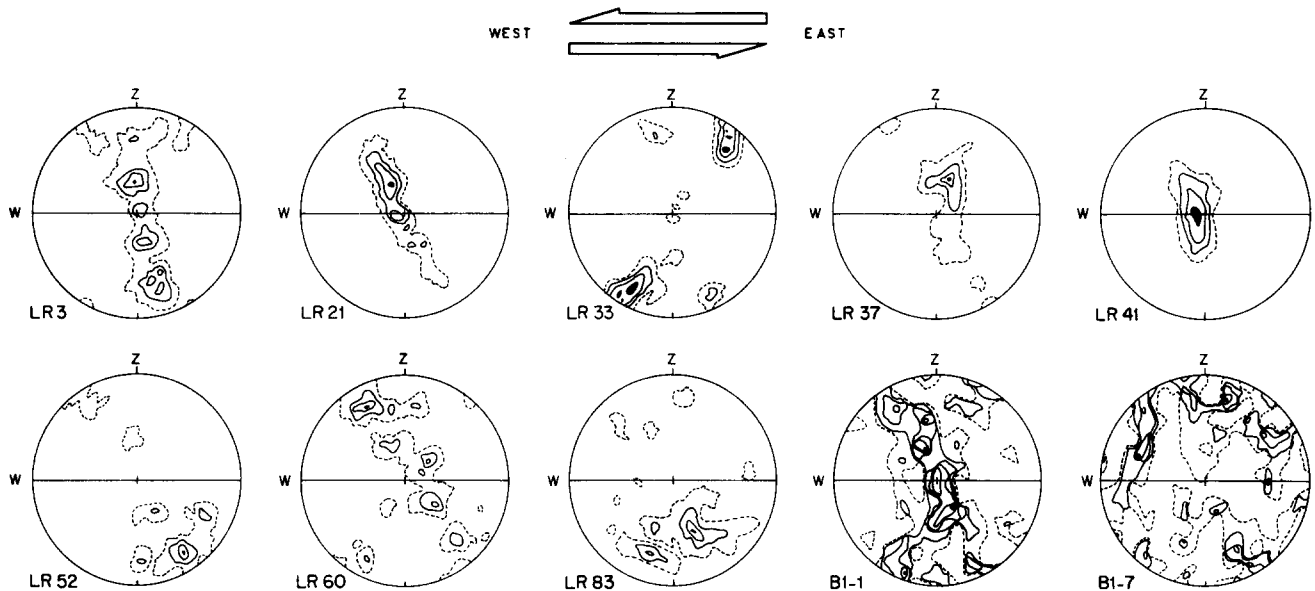


Fig. 5. Quartz (*c*)-axis fabric diagrams in Nevado-Filábride rocks in a composite vertical section through the zone with the planar-linear fabric from bottom (B1-7) to top (LR-3). Locations are shown in Fig. 2. Fabrics of the lower part (B1-7 and B1-1) come from the B section in the western Sierra de los Filabres; fabrics of the higher part (from LR-83 to LR-3) come from the LR section in the central Sierra Nevada. Equal-area, lower-hemisphere projections. LR-3:  $n = 150$  (number of axes); contours at 3, 8, 14 and 20% per 1% of area. LR-21:  $n = 150$ ; 6, 12, 18 and 24%. LR-33:  $n = 150$ ; 5, 10, 15 and 20%. LR-37:  $n = 150$ ; 6, 12, 18 and 24%. LR-41:  $n = 150$ ; 5, 15, 30 and 45%. LR-52:  $n = 150$ ; 4, 9, 14 and 19%. LR-60:  $n = 150$ ; 3, 7, 11 and 15%. LR-83:  $n = 150$ ; 3, 7, 11 and 15%. B1-1:  $n = 100$ ; 1, 2, 3, 4 and 7%. B1-7:  $n = 100$ ; 1, 2, 3, 4 and 7%.

recumbent folds ( $F_p$ ) with amplitudes that vary from a few centimetres to two kilometres. The axial planes of the  $F_p$  folds are gently dipping, like the planar-linear fabric, and their hinge lines are subhorizontal and nearly parallel to the stretching lineation ( $L_p$ ). The axial planes and hinge lines are folded by the  $F_c$  folds and the latest gentle to open folds. Some minor folds (sheath-folds) have curved hinge lines. The minor folds correspond to classes 1C or 3, very near class 2 of Ramsay (1967, p. 365). In the diagram of Hudleston (1973, fig. 12), their shapes range from B to F, and their amplitudes range between 5 and 6. Some of the major folds also have curved hinge lines. Major folds with straight hinge lines are well developed in the western Sierra Nevada (Fig. 6) and define a trend of tight to isoclinal folds with a vergence toward the northwest. The hinge lines have a N30°E trend, and form angles of 20–30° with the stretching lineation ( $L_p$ ). In the western Sierra de los Filabres, major folds with curved hinge lines are recognized, producing eye-like forms in the map outcrops (Fig. 7). There are also folds with straight hinge lines which have a N80°E to N120°E trend and a vergence toward the north. They are subparallel to the stretching lineation.

#### Folds with a crenulation cleavage ( $F_c$ )

These inclined folds have an axial-plane crenulation cleavage of very variable distribution and spacing. The minor folds have an interlimb angle that normally varies between 20° and 60°. The curvature of the hinge lines is also variable, from folds with straight hinges and folds with slightly curved hinges to folds with very curved hinges and dome morphology. The straight hinge lines and slightly curved hinges trend subparallel to the

stretching lineation and describe the same curved pattern as the latter in the Nevado-Filábride outcrops. Locally, the hinge lines are oblique to the stretching lineation, and the  $L_p$  lineation is folded. The folds with slightly curved hinges are the most abundant. These folds and those with straight hinges belong to class 1C of Ramsay (1967) in the competent layers, and to class 3 in the incompetent layers. In the diagram of Hudleston (1973), the shapes of the folds vary between classes C, D, E and F and their amplitudes range from 2 to 5, with a maximum at amplitudes 3 and 4.

In the western Sierra Nevada, the  $F_c$  folds are conjugate and close to open, with amplitudes of less than 100 m. These conjugate folds are superposed on the previous  $F_p$  folds with a type 3 interference pattern (Ramsay 1967, p. 530). The vergence of the  $F_c$  folds varies; some have a vergence towards the southeast, and others have a vergence towards the northwest (Fig. 6, cross-sections). Folds with the same vergence are distributed in domains elongated in a N45°E direction, parallel to the stretching lineation ( $L_p$ ) (Fig. 8). At the borders between the domains, where the two fold systems interfere with each other, are polyclinal folds. The axial surfaces of the southeastward-vergent folds dip toward the northwest, and those of the northwestward-vergent folds dip toward the southeast. The hinge lines of the folds of different vergence are not parallel, and the angle between the two is less than 30°, with the hinges of the southeastward-vergent folds approaching an E–W direction. In a system of two conjugate folds, if the line of intersection of the axial planes of the folds is parallel to the reference folded surface, then the hinges of both folds are parallel, but if the intersection line is oblique to the reference surface, then the hinges of the conjugate

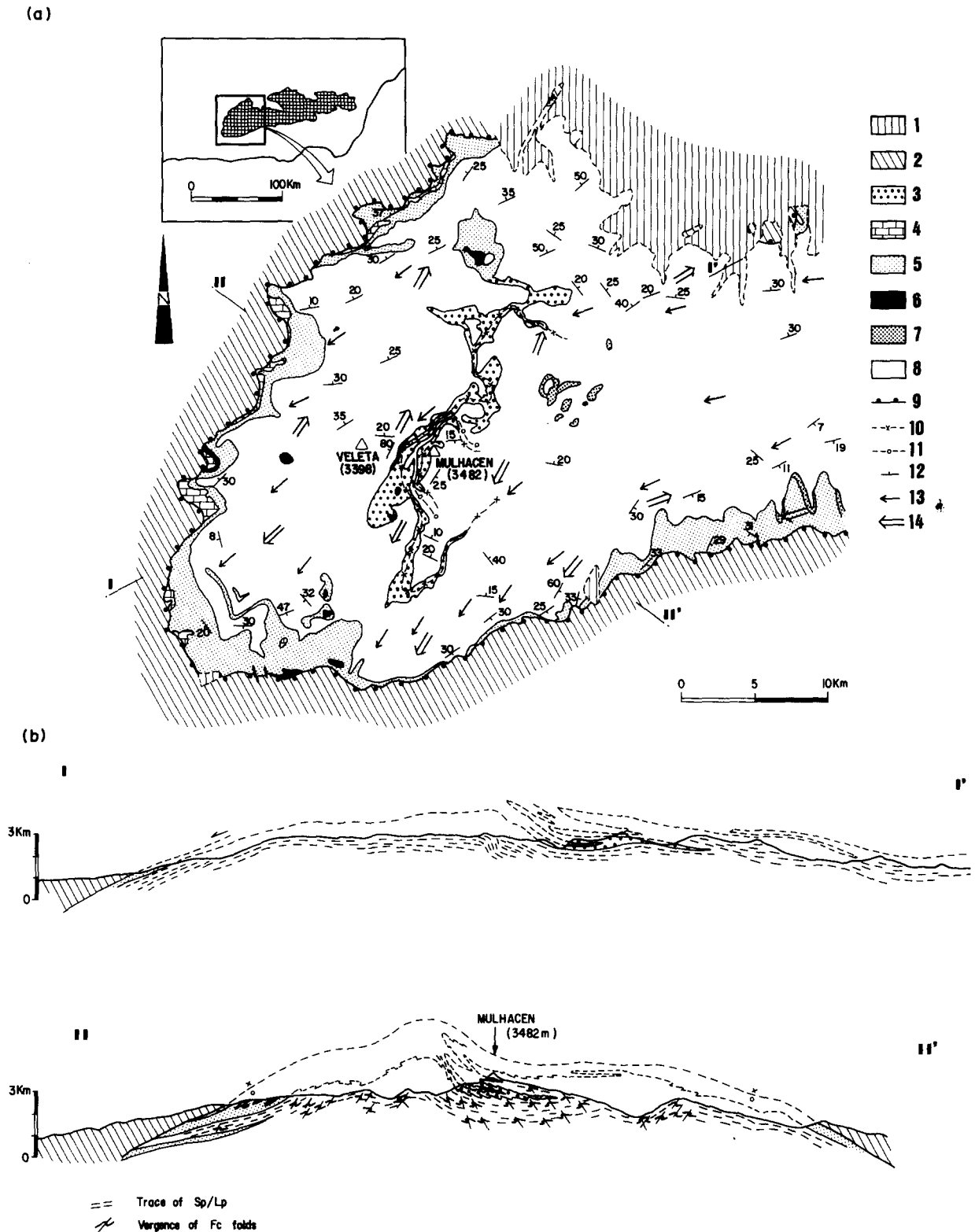


Fig. 6. Geological map and cross-sections of the western Sierra Nevada. 1, Neogene and Quaternary sedimentary rocks; 2, Alpujárride Complex; 3, Tahal Formation, Nevado-Filábride Complex; 4, Las Casas Formation, Nevado-Filábride Complex; 5, Tahal and Las Casas Formations intensely folded with the Montenegro and Aulago Formations; 6, metamorphic igneous rocks; 7, metapsammities of the Aulago Formation; 8, Montenegro Formation; 9, Mecina detachment fault; 10, axial trace of  $F_p$  synclines; 11, axial trace of  $F_p$  anticlines; 12, dip and strike of the  $S_p$  foliation; 13, trend of the  $L_p$  stretching lineation with indication of the sense of movement for the planar-linear fabric; and 14, orientation of  $F_p$  fold hinge lines.



folds have different trends (Tewksbury 1986). This fact implies that in this region, the intersection line of the foliations of the conjugate folds is oblique to the planar linear fabric, and also that the plunge of  $L_p$  towards the southwest is greater than the plunge of the intersection line.

In the western Sierra de los Filabres, the  $F_c$  folds are tight to close folds with amplitudes of less than 1 km. The hinge lines have trends between N60°E and N130°E, and the fold vergence is toward the south. These folds are similar to those described by Platt & Behrmann (1986) in

the Sierra Alhamilla, but with greater amplitudes. The folds are non-cylindrical, with curved hinge lines and relay patterns, and they are transected by the crenulation cleavage ( $S_c$ ). They are superposed on the  $F_p$  folds with straight or curved hinge lines, defining a complex interference pattern (Fig. 7).

#### Late extensional crenulation cleavage

This structure deforms the  $F_c$  folds. It is developed in the upper part of the zone with the planar-linear fabric.

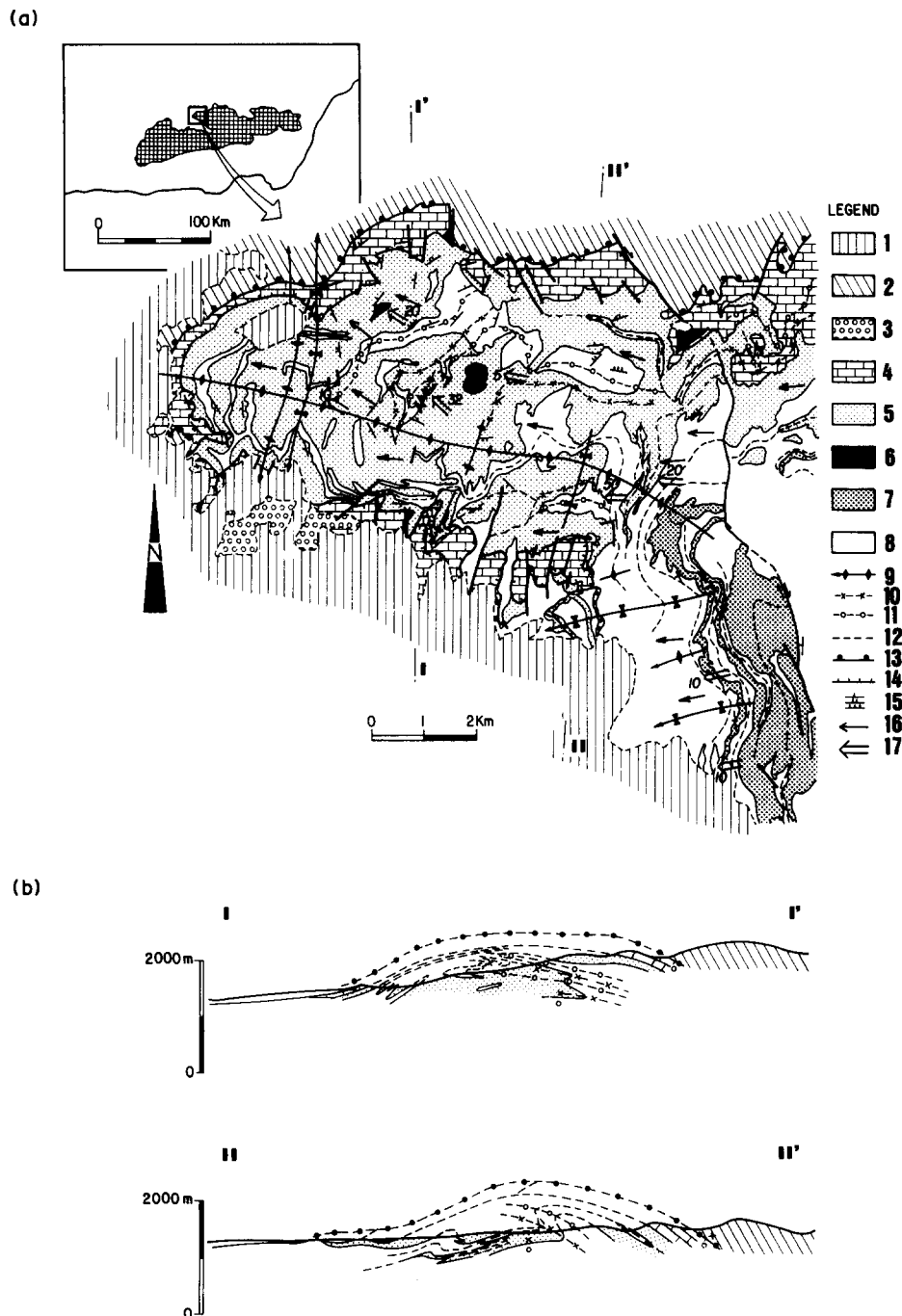


Fig. 7. Geological map and cross-sections of the western Sierra de los Filabres. 1, Neogene and Quaternary sedimentary rocks; 2, Alpujarride Complex; 3, fault rocks; 4, Las Casas Formation, Nevado-Filábride Complex; 5, Tahal Formation, Nevado-Filábride Complex; 6, metamorphic igneous rocks; 7, metapsammities of the Aulago Formation; 8, Montenegro Formation; 9, axial trace of late fold; 10, axial trace of  $F_c$  synform; 11, axial trace of  $F_c$  antiform; 12, axial trace of  $F_p$  fold; 13, Mecina detachment fault; 14, low-angle normal fault; 15, dip and strike of the  $S_p$  foliation: one dip line, 0–30°; two dip lines, 30–60°; three dip lines, 60–90°; 16, trend of the  $L_p$  stretching lineation with indication of the sense of movement for the planar-linear fabric; and 17, orientation of  $F_p$  fold hinge lines.

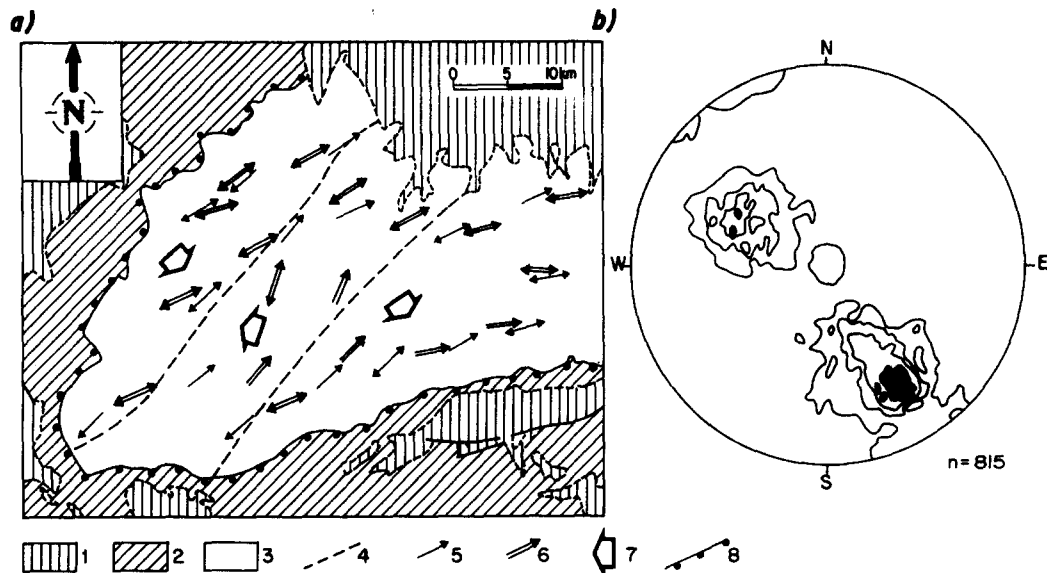


Fig. 8.  $F_c$  fold distribution in the western Sierra Nevada. (a) Geological sketch map showing the distribution of the domains of the  $F_c$  folds with opposite vergence. Orientation of the stretching lineation ( $L_p$ ) is plotted to compare it with the orientation of the  $F_c$  fold hinges. Although they are nearly parallel, the hinges of the  $F_c$  folds with a SE-vergence show a clockwise rotation with respect to  $L_p$ , and the hinges of the  $F_c$  folds with a NW-vergence show an anti-clockwise rotation with respect to  $L_p$ . 1, Neogene and Quaternary sedimentary rocks; 2, Alpujárride Complex; 3, Nevado-Filábride Complex; 4, domain boundaries; 5, orientation of  $L_p$ ; 6, orientation of  $F_c$  fold hinge lines; 7, vergence of  $F_c$  folds; and 8, Mecina detachment fault. (b) Orientation density diagram of the axial-plane cleavage of the  $F_c$  folds. Equal-area, lower-hemisphere projection. Contours at: 1.5, 3, 5, 6, 7 and 8% per 1% of area. The two sets of crenulation surfaces are clearly shown.

This thickness of the materials affected by the late extensional crenulation cleavage varies between 100 and 2000 m from east to west, and is always less than the thickness of the zone with the planar-linear fabric. Two sets of shear surfaces are developed and indicate, respectively, displacements of the hanging wall toward the west-southwest (the most abundant) and toward the east-northeast (less abundant). The latter set is observed only near the detachment surface.

The angle between the shear surface and the tangent plane to the foliation ( $S_p$ ) of the planar-linear fabric at the inflexion line has been measured for both sets of crenulations. This angle is denoted by  $\alpha$  in the set with a top-to-the-west-southwest sense of shearing, and by  $\beta$  in the set with a top-to-the-east-northeast displacement sense. The distributions of  $\alpha$  and  $\beta$  are asymmetric (Fig. 9a & b), with the angles varying between  $10^\circ$  and  $65^\circ$ , maxima at  $40^\circ$ , and angles less than  $40^\circ$  being more frequent than angles greater than  $40^\circ$ . The shear surfaces that form an angle  $\alpha$  or  $\beta$  near  $45^\circ$  cut through those that form a lesser angle. The angle between the conjugate sets of shear surfaces  $\gamma$  ranges between  $90^\circ$  and  $45^\circ$ , and the  $S_p$  foliation is located in the acute angle between the sets. The most frequent value of  $\gamma$  is about  $75^\circ$  and the frequency distribution for  $\gamma$  is also asymmetric (Fig. 9c).

The morphology and the character of the late extensional crenulation cleavage varies in a vertical section (Fig. 9d). In the parts farthest from the detachment surface, the cleavage has a ductile character. This fact makes it difficult to differentiate in outcrop between the late extensional crenulation cleavage and the extensional crenulation cleavage associated with the planar-linear fabric when the  $F_c$  folds are not found. In an intermediate position, the late extensional crenulation

cleavage has a ductile-brittle character, and the spacing between shear surfaces is between 3 and 10 cm. In these zones, the values of angle  $\alpha$  are greater. In the higher parts of a vertical section, near the detachment surface, both conjugate sets are developed and they have a brittle character. Striae can sometimes be observed on their shear planes. The spacing between the microfault planes is less than 3 cm, and values of angles  $\alpha$  and  $\beta$  are greater than in the lower zones.

The direction of the extension is WSW-ENE, as deduced from the striae, the intersection lines between the  $S_p$  foliation and the shear surfaces, and the intersection lines between the two conjugate sets of the late extensional crenulation cleavage. Locally, the two sets of conjugate surfaces coexist, indicating a nearly coaxial strain. The more abundant of the two sets, with a sense of movement of the hanging wall to the west, shows that this structure is generated in a heterogeneous shearing regime.

#### Late deformation

The major structures produced by late deformation are the Mecina detachment fault and great open folds with kilometric wavelengths and an E-W trend. The minor structures are microfaults and joints.

The Mecina detachment fault outcrops in the southeastern Betic Cordillera in a region measuring more than 200 km in length (Fig. 1). The detachment surface, which in some places is parallel and in other places is oblique to the planar-linear fabric, cuts down-section towards the southwest in the footwall. Associated with this surface there are fault gouges in which cataclastic fabrics, trails,  $S-C$  structures, striae and other brittle

structures can be observed. These structures show displacement of the hanging wall (Alpujarride Complex) towards the west in the Sierra Alhamilla, Sierra de los Filabres and northern Sierra Nevada. The displacement is toward the southwest in the southern Sierra Nevada (Fig. 2). Along the detachment fault, there are also fault rocks consisting of a carbonate matrix that includes fragments of the Nevado-Filábride and Alpujarride materials (the Konglomeratische Mergel of Brouwer 1926; the rauhewackes of Leine 1968). This fault rock can be either a mylonite (Martínez-Martínez 1984, Platt *et al.* 1984, Alvarez 1987) or a cataclasite. The sense of movement deduced in this rock is similar to that deduced in the fault gouges.

Microfaults are grouped into several sets: one, composed of faults subparallel to the detachment surface, with movement of the hanging walls towards the west-southwest and another consisting of two conjugate sets of normal faults. These last fault sets have a NW–SE strike, with dips of about 60° towards the northeast and the southwest, respectively. They have fault gouges some centimetres thick and, sometimes, albitic cataclasites.

The joints are systematic tension fractures occasionally filled with quartz, siderite and albite, with openings that can reach 10 cm. Their walls are usually planar and can reveal plumose structures. The joints are subvertical and are grouped in two normal sets. Those of the most developed set have a northwest-southeast strike, and are normal to the stretching lineation. Their mean spacing ranges from 20 cm to 1 m, and their mean length is several metres.

### DEFORMATION IN THE ALPUJARRIDE COMPLEX

The principal ductile deformation generated planar and planar-linear fabrics in the minerals produced by the earlier HP–LT metamorphic event. If the folds that deform them are restored, these fabrics become subhorizontal. Locally, stretching lineations with a ENE–WSW trend are developed with a very heterogeneous intensity. These fabrics are related to ductile thrusts whose hanging walls moved towards the east-northeast (Tubía 1985, Cuevas *et al.* 1986, Cuevas 1988).

A crenulation cleavage that is axial planar to open to close folds is superimposed upon the *S* and *S–L* fabrics. These folds have overturned limbs, subhorizontal hinge lines with a ENE–WSW trend, and amplitudes greater than 1 km. The vergence of the folds can be towards the northwest (Simancas & Campos 1988) or the southeast (Delgado 1978), or the folds can be polyclinal with double vergence (Sanz de Galdeano 1986).

The folds are cut by a system of ductile–brittle and brittle low-angle faults with hanging wall displacement towards the north-northwest and west-southwest. The faults join downward with the detachment surface without penetrating the footwall. Extensional crenulation cleavages and fault gouges are developed in association

with these faults. Several authors have interpreted the faults with a top-to-the-north-northwest sense of movement as thrusts (Simancas & Campos 1988, de Jong 1991), while others have considered them as low-angle normal faults (Cuevas 1988, García-Dueñas & Balanyá 1991). The faults with a top-to-the-west-southwest sense of movement are normal ones, and together with the detachment fault they form the Mecina extensional system (Jabaloy *et al.* 1992).

Later structures include high-angle normal faults, strike-slip faults and joints. The high-angle normal faults are variable in strike. Although there are faults of all possible orientations, sets with N150°E, N45°E and N90°E strikes (Sanz de Galdeano 1983) are observed around the Sierra Nevada and western Sierra de los Filabres. These faults produced an extension with a radial character.

The joints are developed preferentially in the limestones and dolostones. They are systematic tension fractures grouped in three sets that are perpendicular to each other, and they have mean spacings of several centimetres. One of the sets is subhorizontal and the others are subvertical, with NW–SE and NE–SW strikes.

### DISCUSSION

The ductile, ductile–brittle and brittle deformations that are observed in the upper part of the Nevado-Filábride Complex have been produced by heterogeneous shearing. The direction of the main extension is inferred from the stretching lineations, the intersection lines of the conjugate shear surfaces of the late extensional crenulation cleavage, and the striae. It is subhorizontal and trends in an E–W direction, but with a curved pattern. The sense of movement is deduced from the pressure shadows around porphyroblasts, quartz *c*-axis fabrics, *S–C* structures, and other structures. All these structures point to a displacement of the hanging wall towards the west. This sense of movement coincides with that deduced for the Mecina detachment fault. The lower limit of the development of the planar-linear fabric and the detachment surface cuts down across the lithological contacts in the sense of movement, as shown by thinning and omission of the upper Nevado-Filábride rocks. This observation indicates that the detachment acts like a low-angle normal fault. The agreement between the direction and sense of movement, the extensional character and the fact that the deformation by heterogeneous ductile shearing is always located in the footwall, led Galindo-Zaldívar *et al.* (1989) to argue that all the aforementioned structures were generated in one extensional episode. The superposition criteria show that in this extensional episode the planar-linear fabric was the first structure to be generated, followed by the  $F_c$  folds and the late extensional crenulation cleavages.

The extension was produced in rocks that had undergone a previous episode of crustal thickening accompanied by HP–LT metamorphism. The planar-linear

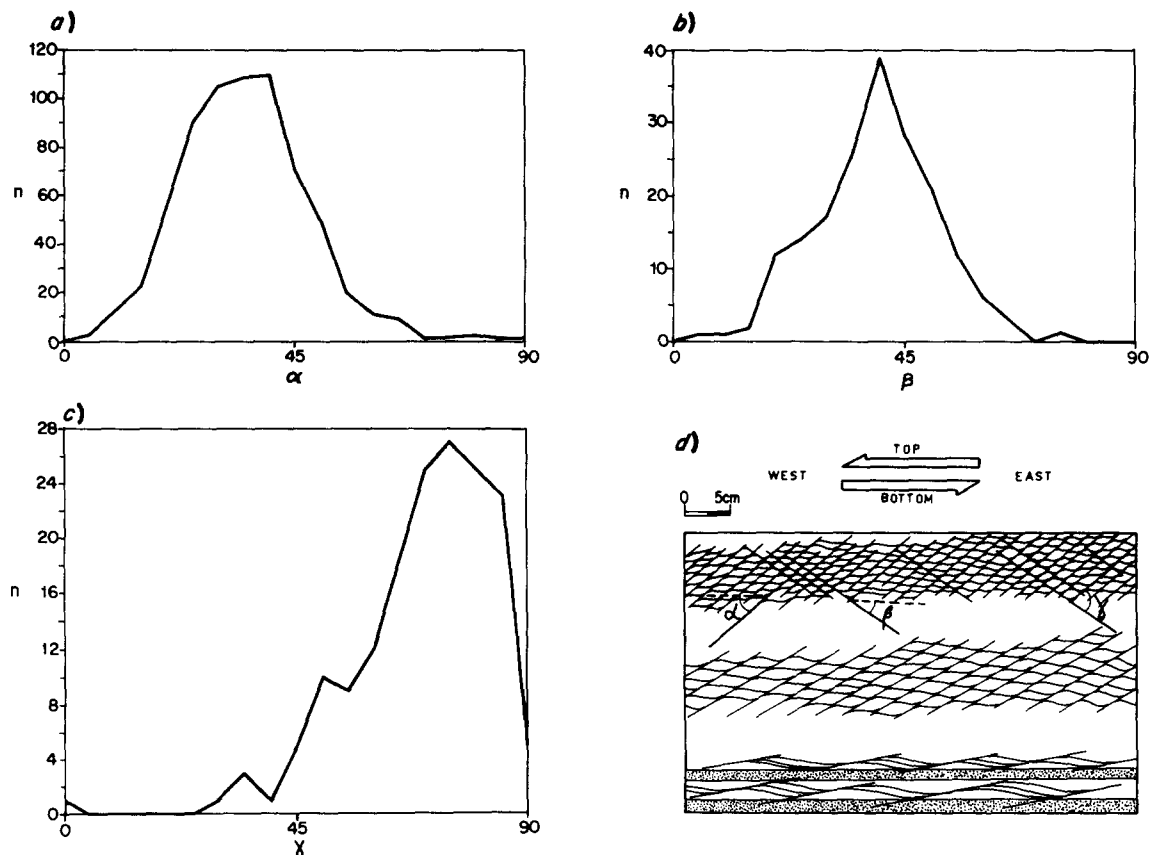


Fig. 9. Frequency distribution diagrams of angles defining the late extensional crenulation cleavage. (a)  $\alpha$  is the angle between the shear surfaces with a top-to-the-west sense of movement and the plane which is tangent to the deformed  $S_p$  foliation at the inflexion line. (b)  $\beta$  is the angle between the shear surfaces with a top-to-the-east sense of movement and the plane which is tangent to the deformed  $S_p$  foliation at the inflexion line. (c)  $\gamma$  is the angle between the conjugate shear surfaces. (d) Sketch of the shape variation of the late extensional crenulation cleavage in a vertical section. The top is closest to the detachment surface; the dotted layers represent metapsammite layers.

fabric associated with the extension overprinted the fabrics generated during the previous episode of crustal thickening, and the minerals formed during the HP-LT metamorphism were also deformed. The intensity of development of the extensional structures does not allow the reconstruction of the previous structures.

The association of the planar-linear fabric with the retrograde greenschist facies assemblages and the zoning of the quartz microstructures suggest that the  $S_p/L_p$  now observed in the upper parts of the complex was generated at a lower temperature and is younger than the  $S_p/L_p$  observed in the lower parts. The variation of the quartz  $\langle c \rangle$ -axis fabrics and the increasing intensity of the planar-linear fabric in an upward sense indicate the concentration of shearing deformation in the upper part of the  $S_p/L_p$  zone.

The fact that the intersection lines between conjugate crenulation foliations of the  $F_c$  folds have the same trend as the stretching lineation, but a different plunge, suggests a rigid rotation of the fabric with respect to the  $F_c$  folds. If the intersection lines are horizontal,  $L_p$  plunges and  $S_p$  dips toward the southwest. Foliation is rotated with respect to the intersection lines in the same shearing sense. This rotation is similar to that proposed in models of extensional systems with isostatic unroofing (Spencer 1984, Wernicke & Axen 1988). In these models, the uplifting of the footwall deforms the extensional shear zone, producing an antiformal fold. The

limb of this antiform that dips in the same direction as the shear zone undergoes rotation in the same sense as that associated with shear in the shear zone.

The cross-cutting relationships of the shear surfaces of the late extensional crenulation cleavage that make different angles with the main foliation ( $S_p$ ) show that they were not formed simultaneously. The shear surfaces with angles  $\alpha$  and  $\beta$  of about  $45^\circ$  are the most abundant and were generated after the surfaces with smaller values of  $\alpha$  and  $\beta$ . This fact explains the asymmetric distributions of  $\alpha$  and  $\beta$  that could be a consequence of the progressive strain in the rock. The surfaces could have formed with an initial angle near  $45^\circ$  (Platt & Vissers 1980), which could be greater if  $S_p$  is folded. They were rotated later as a consequence of the shear strain. The variation in the ductile character of the late extensional crenulation cleavage indicates that this deformation was accompanied by a loss of material ductility. The mechanism can also explain why the distributions of  $\alpha$  and  $\beta$  (Figs. 9a & b) favour angles less than  $45^\circ$ , and, moreover, why  $\sigma_1$  is located in the obtuse angle between the two conjugate shear surfaces, in contrast to the case of brittle faults.

The vertical zonation of the extensional crenulation cleavage (Fig. 9d) is consistent with an upwards increase in strain, a fact that coincides with the progressive loss of ductility in this structure. The progressive increase in  $\alpha$  and  $\beta$  upwards may be a consequence of a lesser rotation

of the younger and more brittle shear surfaces. The development of two brittle conjugate sets near the detachment surface suggests that the pure shear component of strain increased in the final stages of evolution of the shear zone (Platt & Vissers 1980).

In the Nevado-Filábride rocks, after undergoing  $F_c$  folding and the development of the superimposed extensional crenulation cleavage, the planar-linear fabric had generally a lower dip than the detachment surface, which cuts down-section with respect to the planar-linear fabric.

In the Alpujarride rocks, brittle structures (faults and joints) related to the Mecina extensional system are superposed upon ductile structures. These ductile structures show a top-to-the-east-northeast sense of movement for the shear zones. Faults with a top-to-the-west sense of movement are low-angle normal faults with the same movement sense as the Mecina detachment fault, and they contribute to a ENE–WSW extension.

The fast exhumation of the rocks during the thinning process may have produced the joint system that is located preferentially in the Alpujarride limestone and dolostone.

The metamorphic evolution, together with radiometric ages, suggests a rapid uplift and retrograde metamorphism (Monié *et al.* 1991) that is consistent with the above interpretation. In fact, the Alpujarride materials have mineral assemblages that indicate temperatures below 450°C and pressures of up to 10 kbar (Azañón & Goffé 1991), conditions which ended at around 25 Ma. (Monié *et al.* 1991). The HP–LT conditions evolved in the units of the upper part of the Alpujarride Complex to LP–HT conditions at around 500–600°C and 2–4 kbar ending at around 21 Ma (Zeck *et al.* 1989), and the rocks were first eroded in Upper Aquitanian–Lower Burdigalian times (Martín-Algarra 1987). In the rocks of the units of the intermediate and lower part of the Alpujarride Complex, the HP–LT metamorphism evolved to LP–LT conditions in which cookeite is not disequibrated, which implies temperatures below 450°C (Azañón & Goffé 1991) and a geothermal gradient near 48°C km<sup>-1</sup> (Cuevas 1988). This implies final metamorphic pressures near 2–3 kbar. These rocks were cooled below 350°C by 19 Ma (Monié *et al.* 1991) and they first underwent erosion in Middle to Upper Serravallian (Rodríguez-Fernández *et al.* 1990).

The Nevado-Filábride rocks underwent Alpine metamorphism under conditions of 500°C and up to 12 kbar pressure (Gómez-Pugnaire & Fernández-Soler 1987), ending at 48 Ma (Monié *et al.* 1991). This event evolved to a IP–IT metamorphic event, with 550–600°C and 7 kbar (Puga & Díaz de Federico 1976) that ended 23 Ma ago, and the rocks were eroded in Upper Serravallian–Basal Tortonian times. At this point, the Nevado-Filábride rocks were in contact in surface outcrops with Alpujarride rocks that had been subjected to 2–3 kbar of pressure at 19 Ma. These data indicate uplift rates of approximately 2 mm a<sup>-1</sup> for the Nevado-Filábride rocks between 23 and 12 Ma, and approximately 1 mm a<sup>-1</sup> for the Alpujarride rocks between 19 and 12 Ma. Prior to

19 Ma, the Alpujarride rocks had higher uplift rates (around 5 mm a<sup>-1</sup>) which are in agreement with the data of Zeck *et al.* (1989, 1990). In fact, the rocks of the upper part of the Alpujarride Complex that were subjected to pressures up to 10 kbar at 25 Ma were in surface outcrops around 19 Ma. The uplift rates for Lower and Middle Miocene times are different to those obtained by Weijermars (1985), as this author did not take into account the HP–LT metamorphism in the Alpujarride Complex; the uplift rates estimated by Weijermars (1985) in the Messinian–Quaternary time period (0.15–0.1 mm a<sup>-1</sup>), obtained from the data of the Neogene basins, are lower than those of the previous periods. The rates calculated in our study are in agreement with uplift rates deduced in other areas undergoing extension (Fortier & Haudenschild 1991).

## CONCLUSIONS

Extensional deformation in a heterogeneous shear regime, with top-to-the-west-southwest sense of movement, was produced in the Nevado-Filábride and Alpujarride complexes. The contact between the complexes is extensional in nature—the Mecina detachment fault. After a stage of crustal thickening, the extensional regime began at 23 Ma and continues to the present day. Estimated uplift rates for the Alpujarride rocks decrease from 5 (25–19 Ma) to 1 mm a<sup>-1</sup> (19–12 Ma). In the Nevado-Filábride rocks, uplift rates were (2 mm a<sup>-1</sup>) in the 23–12 Ma time period.

Extensional deformation in the Nevado-Filábride rocks (footwall) produced planar-linear fabrics, folds, extensional crenulation cleavages, faults and joints. Brittle and ductile structures were generated in the same shearing regime. The brittle to ductile evolution was a consequence of the pressure and temperature decreasing as a result of unroofing of the footwall. The ductile deformation was constrictive in character. In the extensional regime, tight to open folds ( $F_c$ ) with hinge lines parallel to the stretching lineation were produced. The folds indicate an external rigid rotation of the planar-linear fabric with respect to the zone of the maximum shear strain. This rotation is similar to those proposed in models for the isostatic unroofing of extensional systems.

In the Alpujarride Complex (hanging wall) only brittle structures, faults and joints were developed during the extensional regime. Low-angle normal faults with a top-to-the-west-southwest sense of movement have the same kinematics as the Mecina detachment fault. Alpujarride low-angle faults were active before Tortonian time. High-angle faults, generally with normal slip, were superposed upon the earlier structures in the Tortonian to Quaternary time period.

*Acknowledgements*—We thank J. Andrews, M. Ford and J. P. Platt for their comments and the critical reviews of this manuscript, and also J. A. Azor and E. Fernandez for their comments during discussion of this paper. This study has been financed by the D.G.I.C.Y.T. (Spain) PB90-0860-C03-01 project.

## REFERENCES

- Aldaya, F., Alvarez, F., Galindo-Zaldívar, J., González-Lodeiro, F., Jabaloy, A. & Navarro-Vilá, F. 1991. The Malaguide-Alpujarride contact (Betic Cordilleras, Spain): a brittle extensional detachment. *C. r. Acad. Sci., Paris* **313**, 1447–1453.
- Aldaya, F., Campos, J., García-Dueñas, V., González-Lodeiro, F. & Orozco, M. 1984. El contacto Alpujarrides/Nevalo-Filábrides en la vertiente Meridional de Sierra Nevada. Implicaciones Tectónicas. In: *El Borde mediterráneo español: evolución del orógeno bético y geodinámica de las depresiones neógenas*, Granada, 18–20.
- Alvarez, F. 1987. La tectónica de la Zona Bética en la región de Aguilas. Unpublished Doctoral thesis, University of Salamanca.
- Azañón, J. M. & Goffé, B. 1991. New occurrence of carpholite–kyanite–cookeite assemblages in the Alpujarride Nappes, Betic Cordilleras, SE Spain. *Terra Abs.* **3**, 88.
- Balanyá, J. C. & García-Dueñas, V. 1987. Les directrices structurales du Domaine d'Alborán de part et d'autre du Déroit de Gibraltar. *C. r. Acad. Sci., Paris* **304**, 929–933.
- Behrmann, J. H. 1983. Microstructures and fabric transitions in calcite tectonites from the Sierra Alhamilla (Spain). *Geol. Rdsch.* **72**, 605–618.
- Bemmelen, R. W. Van, 1927. Bijdrage tot de geologie der Betische Ketens in de Province Granada. Doctoral thesis, University of Delft. *D.T.S., Delft* **12**.
- Blumenthal, M. M. 1927. Versuch einer tektonischen gliederung der Betsichen Cordilleren von Central und Südwest (Andalousien). *Ecol. Geol.* **20**, 487–532.
- Bouillier, A. M. & Bouchez, J. L. 1978. Le quartz en rubans dans le mylonites. *Bull. Soc. géol. Fr.* **20**, 253–262.
- Brouwer, H. A. 1926. The structure of the Sierra Nevada. *Proc. Kon. Ned. Akad. Wet.* **29**, 878–882.
- Cuevas, J. 1988. Microtectónica y metamorfismo de los Mantos Alpujarrides del Tercio Central de las Cordilleras Béticas (entre Motril y Adra). Doctoral thesis, University of Pais Vasco. In: *Publicaciones especiales del Boletín Geológico y Minero, I.T.G.E., Madrid*.
- Cuevas, J., Aldaya, F., Navarro-Vilá, F. & Tubía, J. M. 1986. Caractérisation de deux étapes de charriage principales dans les nappes Alpujarrides centrales (Cordillères Bétiques, Espagne). *C. r. Acad. Sci., Paris* **302**, 1177–1180.
- Delgado, F. 1978. Los Alpujarrides en Sierra de Baza (Cordilleras Béticas, España). Unpublished Doctoral thesis, University of Granada.
- Didon, J., Durand-Delga, M. & Kornprobst, J. 1973. Homologies géologiques entre les deux rives du déroit de Gibraltar. *Bull. Soc. géol. Fr.* **15**, 17–115.
- Durand-Delga, M. & Foucault, A. 1967. La Dorsale Bétique, nouvel élément paléogéographique et structural des Cordillères Bétiques, au bord Sud de la Sierra Arana (Prov. de Granada). *Bull. Soc. géol. Fr.* **9**, 223–228.
- Egeler, C. G. 1964. On the tectonics of the Eastern Betic Cordilleras (SE Spain). *Geol. Rdsch.* **58**, 260–269.
- Egeler, C. G. & Simon, O. J. 1969. Orogenic evolution of the Betic Zone (Betic Cordilleras, Spain) with emphasis on the nappe structures. *Geologie Mijnb.* **48**, 296–305.
- Fallot, P. 1948. Les Cordillères Bétiques. *Estud. Geol.* **4**, 83–172.
- Fortier, S. M. & Haudenschild, U. 1991. Rate of unroofing at the South Mountains Metamorphic core complex, Arizona: constraints from Al-in-hornblende geobarometry and K–Ar geochronology. *Geol. Soc. Am. Abs. w. Prog.* **23**, A247.
- Galindo-Zaldívar, J. 1990. Geometría y cinemática de las deformaciones neógenas en Sierra Nevada (Cordilleras Béticas). Unpublished Doctoral thesis, University of Granada.
- Galindo-Zaldívar, J. & González-Lodeiro, F. 1988. Faulting phase differentiation by means of computer search on a grid pattern. *Annales Tectonicae* **2**, 90–97.
- Galindo-Zaldívar, J., González-Lodeiro, F. & Jabaloy, A. 1989. Progressive extensional shear structures in a detachment contact in the western Sierra Nevada (Betic Cordilleras, Spain). *Geodin. Acta* **3**, 73–85.
- Galindo-Zaldívar, J., González-Lodeiro, F. & Jabaloy, A. 1991. Geometry and kinematics of post-Aquitania brittle deformation in the Alpujarride rocks and their relation with the Alpujarride/Nevalo-Filábride contact. *Geogaceta* **10**, 130–134.
- García-Dueñas, V. & Balanyá, J. C. 1986. Estructura y naturaleza del Arco de Gibraltar. *Maleo. Bol. Inf. Soc. Geol. Portugal* **2**, 23.
- García-Dueñas, V. & Balanyá, J. C. 1991. Fallas normales de bajo ángulo a gran escala en las Béticas occidentales. *Geogaceta* **9**, 33–37.
- García-Dueñas, V., Martínez-Martínez, J. M. & Navarro-Vilá, F. 1986. La zona de falla de Torres Cartas, conjunto de fallas normales de bajo ángulo entre Nevalo-Filábrides y Alpujarrides (Sierra Alhamilla, Béticas orientales). *Geogaceta* **1**, 17–19.
- Goffé, B., Michard, A., García-Dueñas, V., González-Lodeiro, F., Monié, P., Campos, J., Galindo-Zaldívar, J., Jabaloy, A., Martínez-Martínez, J. M. & Simancas, J. F. 1989. First evidence of high-pressure, low-temperature metamorphism in the Alpujarride nappes, Betic Cordilleras (SE Spain). *Eur. J. Mineral.* **1**, 139–142.
- Gómez-Pugnaire, M. T. & Cámara, F. 1990. La asociación de alta presión distena + talco + fengita coexistente con escapolita en metapelitas de origen evaporítico (Complejo Nevalo-Filábride, Cordilleras Béticas). *Rev. Soc. Geol. España* **3**, 373–384.
- Gómez-Pugnaire, M. T. & Fernández-Soler, J. M. 1987. High-pressure metamorphism in metabasites from the Betic Cordilleras (SE Spain) and its evolution during the Alpine orogeny. *Contr. Miner. Petrol.* **95**, 231–244.
- González-Lodeiro, F., Orozco, M., Campos, J. & García-Dueñas, V. 1984. Cizallas dúctiles y estructuras asociadas en los Mantos del Mulhacén y Veleta, primeros resultados sobre Sierra Nevada y Sierra de los Filabres. In: *El borde mediterráneo español. Evolución del Orógeno bético y Geodinámica de las depresiones neógenas*, Granada 5–8.
- Hudleston, P. J. 1973. Fold morphology and some geometrical implications of theories of fold development. *Tectonophysics* **16**, 1–46.
- Jabaloy, A. 1991. La estructura de la región occidental de la Sierra de los Filabres (Cordilleras Béticas). Unpublished Doctoral thesis, University of Granada.
- Jabaloy, A., Galindo-Zaldívar, J. & González-Lodeiro, F. 1992. The Mecina extensional system: their relation with the post-Aquitania piggy-back basins and the paleostress evolution (Betic Cordilleras, Spain). *Geomar. Lett.* **12**, 96–103.
- Jabaloy, A. & González-Lodeiro, F. 1988. La deformación en los bloques de techo y muro de los cabalgamientos de las unidades inferiores Nevalo-Filábrides (Cordilleras Béticas, SE España). *Estud. Geol.* **44**, 253–261.
- Jong, K. De, 1991. Tectono-metamorphic studies and radiometric dating in the Betic cordilleras (SE Spain)—with implications for the dynamics of extension and compression in the western Mediterranean area. Unpublished Doctoral thesis, University of Amsterdam.
- Krogh, E. J. & Råheim, A. 1978. Temperature and pressure dependence of Fe–Mg partitioning between garnet and phengite, with particular reference to eclogites. *Contr. Miner. Petrol.* **66**, 75–80.
- Lafuste, M. J. & Pavillon, M. J. 1976. Evidence d'Eifélien daté au series des terrains métamorphiques des Zones Internes des Cordillères Bétiques. Intérêt de ce nouveau repère stratigraphique. *C. r. Acad. Sci., Paris* **283**, 1013–1018.
- Langenberg, C. W. 1972. Polyphase deformation in the eastern Sierra de los Filabres, North of Lubrin, SE. Spain. (Doctoral thesis, University of Amsterdam.) In: *GUA Pap. Geol., Ser. 1*, 2.
- Leine, L. 1968. Rauhswackes in the Betic Cordilleras, Spain. Nomenclature, description and genesis of weathered carbonate breccias of tectonic origin. Unpublished Doctoral thesis, University of Amsterdam.
- Martín-Algarra, A. 1987. Evolución geológica alpina del contacto entre las Zonas Internas y las Zonas Externas de la Cordillera Bética. Unpublished Doctoral thesis, University of Granada.
- Martínez-Martínez, J. M. 1984. Evolución tectono-metamórfica del Complejo Nevalo-Filábride en el sector de unión entre Sierra Nevada y Sierra de los Filabres, Cordilleras Béticas (España). (Doctoral thesis, University of Granada.) In: *Cuadernos de Geología de la Universidad de Granada* **13**.
- Martínez-Martínez, J. M. 1985. Las sucesiones Nevalo-Filábrides en la Sierra de los Filabres y Sierra Nevada. Correlaciones. *Cuadernos de Geología de la Universidad de Granada* **12**, 127–144.
- Massone, H. J. & Schreyer, W. 1987. Phengite geobarometry based on the limiting assemblage with K-feldspar, phlogopite, and quartz. *Contr. Miner. Petrol.* **96**, 212–224.
- Mellini, M., Nieto, F., Alvarez, F. & Gómez-Pugnaire, M. T. 1991. Mica–chlorite intermixing and altered chlorite from the Nevalo-Filábride micaschists, Southern Spain. *Eur. J. Mineral.* **3**, 27–38.
- Monié, P., Galindo-Zaldívar, J., González-Lodeiro, F., Goffé, B. & Jabaloy, A. 1991. First report on  $^{40}\text{Ar}/^{39}\text{Ar}$  geochronology of alpine tectonics in the Betic Cordilleras (Southern Spain). *J. geol. Soc. Lond.* **148**, 289–297.
- Nijhuis, H. J. 1964. Plurifacial alpine metamorphism in the south-eastern Sierra de los Filabres. South of Lubrin, SE Spain. Unpublished Doctoral thesis, University of Amsterdam.
- Platt, J. P. 1986. Dynamics of orogenic wedges and the uplift of

- high-pressure metamorphic rocks. *Bull. geol. Soc. Am.* **97**, 1037–1053.
- Platt, J. P. & Behrmann, J. H. 1986. Structures and fabrics in a crustal-scale shear zone, Betic Cordillera, SE Spain. *J. Struct. Geol.* **8**, 15–33.
- Platt, J. P., Behrmann, J. H., Martínez, J.-M. M. & Vissers, R. L. M. 1984. A zone of mylonite and related ductile deformation in the Alpujarride nappe complex, Betic Cordilleras, S. Spain. *Geol. Rdsch.* **73**, 773–785.
- Platt, J. P. & Vissers, R. L. M. 1980. Extensional structures in anisotropic rocks. *J. Struct. Geol.* **2**, 379–410.
- Platt, J. P. & Vissers, R. L. M. 1989. Extensional collapse of thickened continental lithosphere: A working hypothesis for the Alborán sea and Gibraltar arc. *Geology* **17**, 540–543.
- Puga, E. & Díaz de Federico, A. 1976. Metamorfismo polifásico y deformaciones alpinas en el Complejo de Sierra Nevada, implicaciones geodinámicas. In: *Reunión sobre la Geodinámica de las Cordilleras Béticas y del Mar de Alborán, Granada* 79–111.
- Ramsay, J. G. 1967. *Folding and Fracturing of Rocks*. McGraw-Hill, New York.
- Rodríguez-Fernández, J., Sanz de Galdeano, C. & Serrano, F. 1990. Le couloir des Alpujarras. *Docum. trav. IGAL* **12/13**, 87–100.
- Sanz de Galdeano, C. 1983. Los accidentes y fracturas principales de las Cordilleras Béticas. *Estud. Geol.* **39**, 157–165.
- Sanz de Galdeano, C. 1986. Structure et stratigraphie du secteur oriental de la Sierra Almiéjara (Zone Alpujarride, Cordilleres Bétiques). *Estud. Geol.* **42**, 281–289.
- Simancas, J. F. & Campos, J. 1988. La estructuración de componente norte de los Mantos Alpujarrides en el sector central de la Cordillera Bética. In: *Simposio sobre Cinturones Orogénicos. II Congreso Geológico de España. S.G.E. Granada*, 27–33.
- Soto, J. I., García-Dueñas, V. & Martínez-Martínez, J. M. 1990. Valor de la deformación dúctil asimétrica en el ortogneis de Lubrín (Manto de Bedar-Macael, Complejo Nevado-Filábride, Béticas). *Geogaceta* **7**, 92–94.
- Spencer, J. F. 1984. Role of tectonic denudation in warping and uplift of low-angle normal faults. *Geology* **12**, 95–98.
- Tewksbury, B. J. 1986. Conjugate crenulation cleavages in the Uncompahgre Formation, Needle Mountains, Colorado. *J. Struct. Geol.* **8**, 145–155.
- Torres-Roldán, R. L. 1979. La evolución tectonometamórfica del macizo de Los Reales. (Extremo occidental de la zona Bética). Unpublished Doctoral thesis, University of Granada.
- Tubía, J. M. 1985. Sucesiones metamórficas asociadas a rocas ultramáficas en los Alpujarrides occidentales (Cordilleras Béticas, Málaga). Unpublished Doctoral thesis, University of País Vasco.
- Vissers, R. L. M. 1981. A structural study of the Central Sierra de los Filabres (Betic Zone, SE Spain), with emphasis on deformational process and their relation to the Alpine metamorphism. *GUA Pap. Geol. Ser.* **1**, 15.
- Weijermars, R. 1985. Uplift and subsidence history of the Alborán basin and a profile of the Alborán diapir (W-Mediterranean). *Geologie Mijnb.* **64**, 349–356.
- Wernicke, B. & Axen, G. J. 1988. On the role of isostasy in the evolution of normal fault systems. *Geology* **16**, 848–851.
- Zeck, H. P., Albat, F., Hansen, B. T., Torres-Roldán, R. L., García-Casco, A. & Martín-Algarra, A. 1989. A  $21 \pm 2$  Ma age for the termination of the ductile Alpine deformation in the internal zone of the Betic Cordilleras. (South Spain). *Tectonophysics* **169**, 215–220.
- Zeck, H. P., Monié, P., Villa, I. & Hansen, B. T. 1990. High uplift and cooling rates in the Betic Cordilleras, South Spain. In: *IX R.C.M.N.S. Congress, Barcelona, 1990 Abs.* 377.
- Zevenhuizen, W. A. 1989. Quartz fabrics and recumbent folds in the Sierra de los Filabres (SE-Spain). *Geodin. Acta* **3**, 95–105.